CHEMISTRY
A EUROPEAN JOURNAL

FULL PAPER

DOI: 10.1002/chem.200((will be filled in by the editorial staff))

Reversible Binding of Solvent to Naked Pb^{II} Centers in Unusual Homoleptic Alkynyl Based $\{Pt_2Pb_2\}$ Clusters

Jesús R. Berenguer, Julio Fernández*, Belén Gil, Elena Lalinde* and Sergio Sánchez.[a]

Abstract. We report a series of luminescent sandwich-type clusters $[Pt_2Pb_2(C{\equiv}CR)_8]$ (R = Tol **1**, C_6H_4OMe-3 **2**, C_6H_4OMe-4 **3**) with a dynamic Pt_2Pb_2 metallic core, which is key in their intriguing stimuli-responsive photophysical properties. The solvent-free solids **1-3** display an orange emission ascribed to charge transfer from Pt-alkynyl fragments to a delocalized orbital with mixed $Pt_2Pb_2/C{\equiv}CR$ nature, having predominant lead contribution and Pb···Pb bonding character (^{3}MLCCT/^{3}IL). They exhibit reversible and nake-eye perceivable mechanical color and luminescence changes attributed to small inter and intramolecular structural modifications induced by gently grinding. Interestingly, **1** and **2** also exhibit a remarkable and fast reversible vapochromic response to donor solvent vapors (acetone, THFMe-2 *yellow*; NCMe *green vs.* dry solids *orange*). The structures of **1(acetone)$_2$**·2(Me_2CO), **2(acetone)$_3$** and **2(THFMe-2)$_2$**, allow to ascribe the vapochromic responses to a fast creation/disruption of solvate clusters $[Pt_2Pb_2(C{\equiv}CR)_8S_x]$ ($x \geq 2$) with concomitant electronic and geometrical modifications within the Pt_2Pb_2 core, which are easily accessible by a slight change of the stereochemical activity of the lone pair. The binding of one (or two) solvent molecules to the Pb^{2+} increases the Pb···Pb separation in the metallic core, causing a destabilization of the target orbital and a larger energy gap of the transitions. All solvates exhibit a remarkable rigidochromism upon lowering the temperature, which is also associated to a gradual increase of the transannular Pb···Pb separation, as revealed by X-ray crystallography of **1(acetone)$_2$** at different temperatures. Investigation of the crystal lattice of **1**·CH_2Cl_2 and **3**·$2CH_2Cl_2$ further suggests that the lack of vapor stimuli response of complex **3** could be attributed to the presence of competitive additional secondary intermolecular Pb···O(OMe) contacts, which gives rise to a more compact network built up from extended chains of clusters.

Keywords: Lead • Platinates • Clusters • Alkynyl • Luminescence • Solvent effects

Introduction

The design and study of new luminescent materials has become a field of increasing interest, not only for the basic understanding of the excited state properties, but also for their practical applications in the development of optoelectronic devices.[1] In this area, the rich σ/π bonding versatility of the alkynyl ligands, complemented with non-covalent metallophilic interactions between closed shell metal ions, have been extensively used as powerful tools for the assembly of homo and heteropolynuclear complexes, having fascinating structures and attractive emissive properties.[1c, 2] The interest in this topic is reflected in the number of review articles dealing with synthetic, structural, photophysical and potential applications (light emitting devices, catalyst, sensing…) of these complexes.[1c, 2-3] By and large, the more extensively studied systems are those involving d^{10}-d^{10} (Cu^I, Ag^I, Au^I, Hg^{II})[1c, 3-4] and, to a lesser extent, d^8(Pt^{II})-d^{10} transition metal ions,[1c, 2, 5] mainly because these metals form relatively strong σ and/or η^x bonding with the alkynyl entities, providing robust polynuclear organometallic networks. Their photophysical properties are primarily determined by the electronic characteristics of the alkynyl σ/π groups, modulated by the strength of the η···(M) alkyne bonds, and the metal-metal interactions in the final aggregate. Notably, some of these complexes have shown strong room-temperature (fluid, solid) phosphorescence[4a, 6] and, in a few occasions, concentration or solvent induced polymorphism and vapochromic accompanied by large changes in the photophysical properties.[4b]

In this area, heteropolynuclear complexes incorporating other borderline post-transition closhed-shell ions have been less explored, because the lower tendency of these metals to be complexed by π alkyne interactions. By using alkynyl platinates as starting bulding

[a] Jesús R. Berenguer, Julio Fernández, Belén Gil, Elena Lalinde and Sergio Sánchez.
Departamento de Química – Centro de Investigación en Síntesis Química.
Universidad de La Rioja, 26006, Logroño, Spain.
E-mail: elena.lalinde@unirioja.es. juliofernandez50@gmail.com

Supporting information for this article is available on the WWW under http://www.chemeurj.org/ or from the author.

blocks, our group has successfully prepared and investigated several families of polynuclear Pt-M aggregates incorporing Cd^{II}[7] and Tl^{I}.[8] The topology and bonding characterization of the final aggregates is usually less predictable and appear to be controlled by the preference of the heterometal (Cd^{II}, Tl^{I}) for the basic Pt^{II} center or for the electron rich alkynyl units, which depend on several factors such as geometry around Pt and alkynyl substituents. Interestingly, some of these systems were found to show drastic color and emission changes[8d] in response to external stimuli such as acetone (vapochromism) or pressure (mechanochroism), likely derived from $Tl^{I}\cdots$solvent contacts or subtle changes in the Pt$\cdots$Tl and Tl$\cdots$alkynyl bonding interactions

In contrast to d^{10} or Tl^{I} ions, the participation of Pb^{II} in metallophilic interactions is notably sparse[9] and, in particular, its potential in the construction of polynuclear networks, supported by alkynyl (σ or π) ligands, have been rarely investigated.[10] We noted that despite the environmental concern of lead, its chemistry has attracted much attention in recent years, not only because of the intriguing structural motifs,[11] caused by the tuning of the electrochemical activity of the lone pair, but also because of its applications in non-linear optics,[12] birrefringent,[13] ferroelectric,[14] semiconductivity[15] and luminescent materials.[9b, 9e-h, 16]

The relationship between the stereochemical activity of the lone pair, the nature of the ancilliary ligands and the resulting rich geometries around Pb^{II}, categorized as hemi or holodirected, have been studied by several authors.[17] It has been stated that coordination of basic and hard ligands induce more mixing of the 6s and 6p orbitals, leading to hemidirected structures with lower coordination numbers, while symmetrical holodirected environment are usually found with high coordination numbers (8-9).[18] The stereochemical activity has mainly related with structural data and little is known about its role in the optical properties of lead based systems.[17] It is now well established that solid state emitting behavior strongly depend on the local molecular structure and the extended arrangement controlled by weaker (metallophilic, metal-solvent, hydrogen bonding, $\pi\cdots\pi$ staking) interactions, which, in some systems, can be reversible changed and tuned by means of external stimuli.[19] In this context the flexibility of Pb^{II} may allow, through different degrees of activity of the lone pair, subtle modifications in the structure making lead containing complexes to have sensing behavior.[19a-c]

In 2008, we found that $[\{Pt(C\equiv CTol)_4\}_2Pb(OH_2)_2]^{2-}$ showed reversible color and emission change upon exposure to acetone. Unfortunately, the low stability of this complex and the lack of suitable solvate crystals for an X-ray study precluded us to study the nature of this behavior.[10] In this contribution, we report the preparation and structural characterization of novel intensely luminescent neutral tetranuclear $[Pt_2Pb_2(C\equiv CR)_8]$ clusters, which display, not only vapochromic response to small donor solvents, but also mechanochromic properties associated to the remarkable flexibility of the lead centers. In this context, it is worth noting that materials able to respond to more than one external stimulus are attracting considerable interest.[19-20] In addition, Time Dependent Density Functional Theory (TD-DFT) calculations were carried out on some selected solvated and unsolvated derivatives to get insight into the nature of their photophysical properties.

Results and Discussion

Synthesis and characterization. Solvent-free clusters $[Pt_2Pb_2(C\equiv CR)_8]$ (R = Tol **1**; C_6H_4OMe-3 **2**; C_6H_4OMe-4 **3**) were obtained by reaction of $(NBu_4)_2[Pt(C\equiv CR)_4]$ with one equivalent of $Pb(ClO_4)_2\cdot 3H_2O$ in acetone. Interestingly, **1** and **2** precipitate as bright-yellow microcrystalline solids but their color and luminescence changes rapidly (~5 min **1**; <1min **2**) to orange, similar to **3**, when the solids are air dried. As discussed below, these changes are related with the loss of acetone solvent molecules when the solids are air dried. The clusters were characterized by standard analytical and spectroscopic techniques and its integrity in solution also supported by $^{195}Pt\{^1H\}$ spectroscopy. Thus, the $^{195}Pt\{^1H\}$ spectra of **1** and **2** reveals the presence of a singlet (δ -3463 **1**, -3488 **2**), shifted in relation to the corresponding precursor ($[Pt(C\equiv CR)_4]^{2-}$ δ -4187 R = Tol; -4167 ppm, R = C_6H_4OMe-3), and flanked by ^{207}Pb satellites ($^1J^{195}_{Pt\text{-}}{}^{207}_{Pb}$ = 2529 Hz **1**; 2363 Hz **2**) with the expected ratio (see Figure 1) for a Pt_2Pb_2 aggregate.[21] The values of the platinum-lead coupling constants are remarkably higher to that reported for [(OAc)Pb(crown-P_2)Pt$(CN)_2$]OAc (274 Hz),[9g] indicating that the involved Pt-Pb bonding is noticeably stronger.

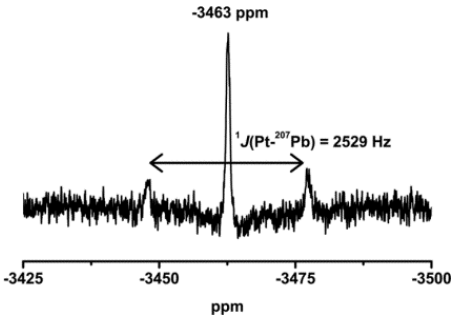

Figure 1. $^{195}Pt\{^1H\}$NMR spectra of **1** in CD_2Cl_2 at 223K.

X-ray structures: Slow diffusion of hexane or diisopropylether into a CH_2Cl_2 solution of **1** (-30ºC) and **3** (4ºC) yielded orange crystals of stoichiometry $[Pt_2Pb_2(C\equiv CTol)_8]\cdot CH_2Cl_2$ and $[Pt_2Pb_2(C\equiv CC_6H_4OMe\text{-}4)_8]\cdot 2CH_2Cl_2$, respectively. Fortunately, for **1**, yellow crystals from acetone of stoichiometry $[\{Pt_2Pb_2(C\equiv CTol)_8\}\cdot 2(Me_2CO)\cdot 2(Me_2CO)]$, **1(acetone)$_2$**$\cdot 2(Me_2CO)$ were also obtained. However, for **2**, suitable crystals were only obtained in acetone ($[Pt_2Pb_2(C\equiv CC_6H_4OMe\text{-}3)_8]\cdot 3(Me_2CO)$, **2(acetone)$_3$**) and THFMe-2 ($[Pt_2Pb_2(C\equiv CC_6H_4OMe\text{-}3)_8]\cdot 2$THFMe-2, **2(THFMe-2)$_2$**). Table S1 shows the most important crystallographic information. The crystal structures are depicted in Figures 2-5 S1-S2 and the most relevant bond lengths and angles are summarized in Table S2. Selected intermetallic distances and angles associated to the metallic core are presented in Table 1.

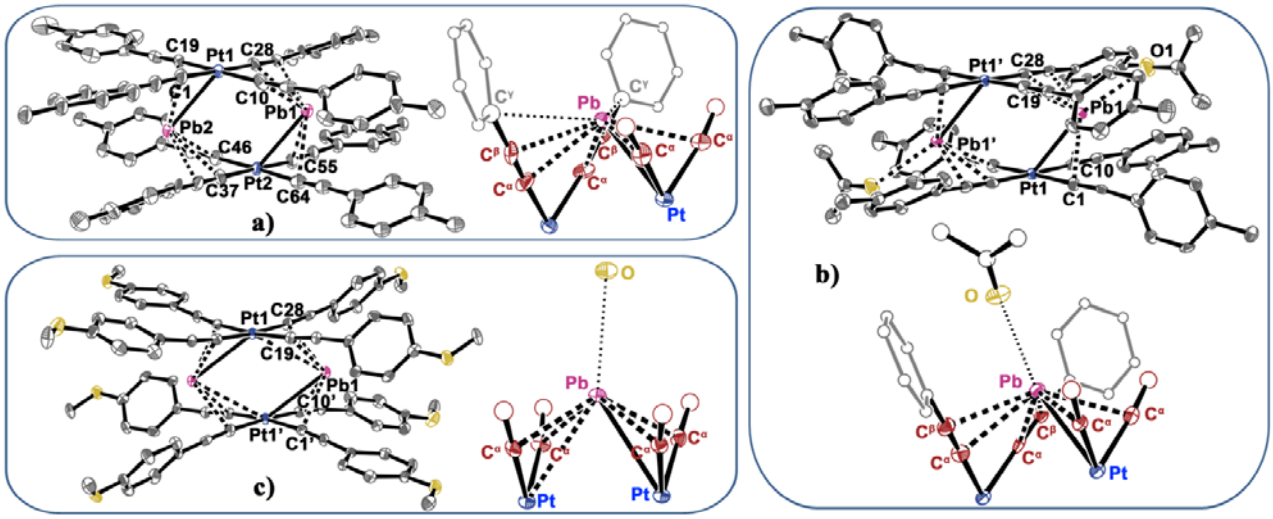

Figure 2. ORTEP views (detailed view of the coordination sphere of lead centers in the insets) of **1**·CH_2Cl_2 (**a**), **1(acetone)$_2$**·2(Me_2CO) (**b**) and **3**·2CH_2Cl_2. Ellipsoids are drawn at 50% probability level. Hydrogen atoms and crystallization solvent molecules are omitted for clarity.

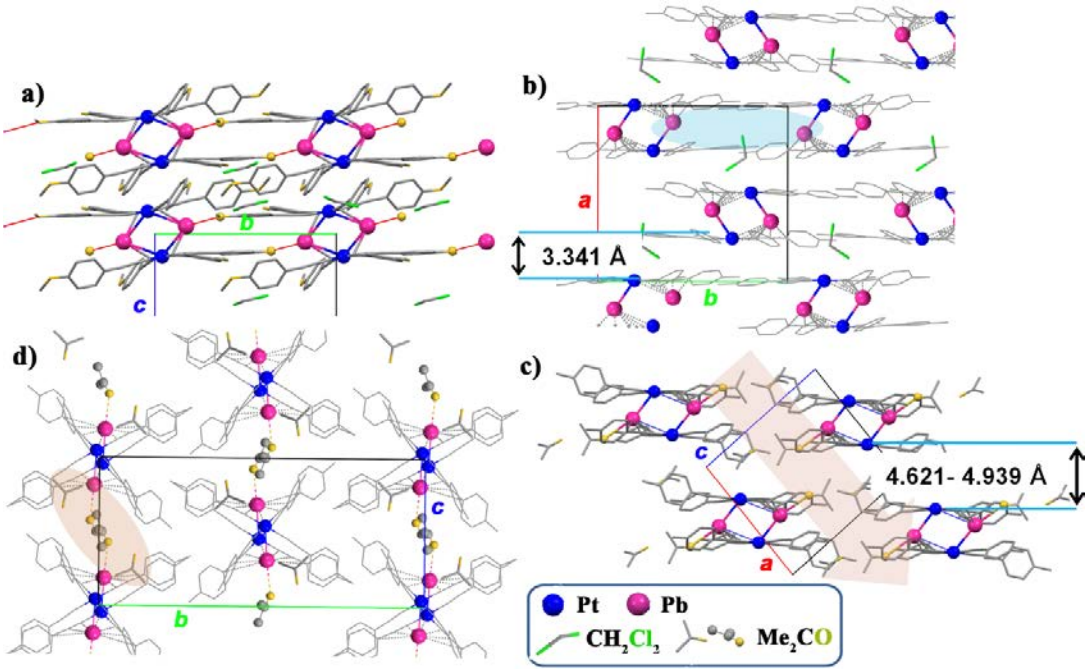

Figure 3. Crystal packing of **3**·CH_2Cl_2 along the *a* axis (**a**). Crystal packing of **1**·2CH_2Cl_2 along the *c* axis (**b**). Crystal packing of **1(acetone)$_2$**·2(Me_2CO) along the *b* axis (**c**) and the *a* axis (**d**).

All complexes display a rare planar rhomboidal Pt_2Pb_2 structural motif supported by platinum-lead and lead-alkynyl bonds. In this context, it is worth noting that only a few bimetallic (Pt-Pb)[9c, 9g, 22] and trimetallic ($Pt^{II}{}_2Pb^{II}$ and $Pt^0Pb^{II}Pt^0$)[9d, 23] compounds incorporating Pt-Pb bonds have been reported and, as far as we know, these complexes are the first examples containing a tetranuclear platinum-lead framework.

The key difference between the CH_2Cl_2 crystallized complexes **1** and **3**, what explains their different behavior towards solvents, is observed in the crystal packing (Figure 3). As can be seen in Figure 3a, in the *p*-methoxyalkynyl derivative **3** the aggregates are joined by two long intermolecular Pb···O(OMe) (3.340 Å),[24] contacts, to form chains which further interconnect by secondary interactions giving rise to a compact network. This Pb···O interaction and the compact packing are likely responsible of its non vapochromism response and also low solubility in usual organic solvents. By contrast, **1** (Figure 3b) displays a lesser compact layer-like arrangement supported by weak interactions between clusters (Figure S1) which leaves empty channels limited by Pb^{II} centers of neighboring clusters along the *b* and *c* axes. This network explains the ease absorption of acetone and others donor solvents, that probably fills this space modifying slightly the local environment of the Pb^{II} ions. As illustration, two views of the extended packing of the solvate **1(acetone)$_2$**·2(Me_2CO) are also represented in Figures 3c,d, showing that the acetone molecules are located along these channels. It is worth noting that the incorporation of the solvent increases the separation between clusters of neighboring sheets (range 4.621 to 4.939 Å in **1(acetone)$_2$** *vs.* 3.341 Å in **1**), giving rise to a less tight packing, which has a positive influence on the emission efficiency[25] as commented below. As in the *p*-methoxyphenyl derivative **3**, in this solvate, each Pb^{II} center is involved in weak bonding contact with only one acetone (Pb···O1 = 2.918(5) Å). The second acetone is acting as crystallization solvent.

The structural details of **1** and **3** reflect the flexibility of the metallic core (Figure 2, Table 1). The platinum units are parallel and eclipsed in **3**, whereas they are found displaced (by 1.62 Å)

retaining an eclipsed disposition in **1**. As a consequence, the Pt_2Pb_2 array, which display two short and two longer Pt···Pb distances, is clearly more asymmetrical in **1** (Figure 2a). The shortest Pt-Pb distances (2.8187(8), 2.8246(8) Å **1**; 3.0852(3) Å **3**) are close to the sum of the covalent radii (2.82 Å), whereas the two other separations are significantly longer, particularly in complex **1** (3.5631(7), 3.5658(7) Å **1**; 3.3555(4) Å **3**), but still below the sum of the van der Waals radii (3.77 Å). As expected, the *transannular* Pt···Pt separation is notably shorter in the eclipsed cluster (3.5838(3) Å **3** *vs.* 3.9286(7) Å **1**), while the Pb···Pb is slightly longer (5.3583(4) **3** *vs.* 5.0893(7) Å **1**). It is worth noting that, while the Pt···Pt distances are in the upper range to those seen in linear chain Pt^{II} complexes (3.01-3.75 Å),[5e, 26] the Pb···Pb are out of the van der Waals limit (4.04 Å). The Pb centers complete their coordination being bonded to four alkynyl entities. In the less asymmetrical derivative **3**, the observed Pb···alkynyl bonding takes place mainly with the C^{α} atoms (Pb-C^{α} 2.592(7)-2.715(7) Å). However, in **1** the two alkynyl ligands associated to the very long Pt-Pb distance exhibit a more symmetrical η^2 bonding (Pb-C^{α} 2.69(2)-2.72(2) Å; Pb-C^{β} 2.74-2.83(2) Å). Curiously, in **1**, the aromatic tolyl rings of η^2-coordinating alkynyl ligands are slightly tilting towards the lead centers (Pb-C^{ipso} // C^{ortho} = 3.47(2)-3.55(2) // 3.72(2)-3.83(2)), presumably reducing somewhat the relatively strong *hemidirected* four-coordinate square-pyramidal environment of the Pb with the active lone pair at the apex of the pyramid.

Table 1: Intermetallic lengths [Å] and angles [deg] [esd] for **1**·CH_2Cl_2, **1(acetone)$_2$**·2(Me_2CO), **2(acetone)$_2$**, **2(acetone)$_4$**, **2(THFMe-2)$_2$** and **3**·$2CH_2Cl_2$.

		Pt-Pb		Pt···Pt	Pb···Pb	Pt-Pb-Pt	Pb-Pt-Pb
		Short	Long				
1		2.8216[a]	3.5644[a]	3.9286(7)	5.0893(7)	74.92[a]	105.08[a]
1(act)$_2$	120	2.8663(3)	3.5834(3)	3.9034(3)	5.1842(3)	73.54(1)	106.46(1)
	200	2.8649(3)	3.5708(3)	3.9176(3)	5.1545(3)	74.08(1)	105.92(1)
	250	2.8639(6)	3.5584(6)	3.9240(7)	5.1313(5)	74.44(2)	105.56(2)
2(act)$_2$		3.0570(5)	3.3519(5)	3.8034(5)	5.1666(5)	72.64(1)	107.36(1)
2(act)$_4$		3.1979(4)	3.3117(5)	3.5830(5)	5.4360(5)	66.77(1)	113.23(1)
2(THFMe-2)$_2$		3.0476(4)	3.4898(4)	3.7220(3)	5.3928(4)	69.02(1)	110.98(1)
3		3.0852(3)	3.3555(4)	3.5838(3)	5.3583(4)	67.47(1)	112.53(1)

[a] Average distance.

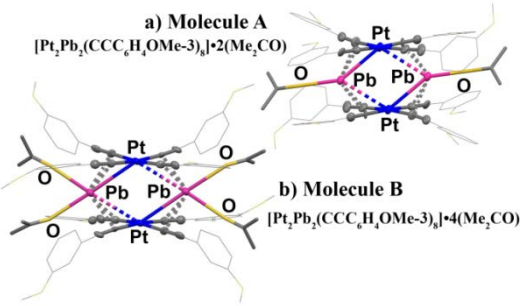

Figure 4. Simplified molecular structure of (**a**) Molecule A [Pt_2Pb_2(C≡CC_6H_4OMe-3)$_8$]·2(Me_2CO) **2(acetone)$_2$** and (**b**) Molecule B **2(acetone)$_4$** found in **2(acetone)$_3$**.

In contrast to that observed in the packing, the X-ray analysis of **1(acetone)$_2$**·2(Me_2CO), at the same temperature to that **1**·CH_2Cl_2 (120K), reveals that the weak interaction of the acetone molecules with the Pb^{II} centers causes a minor impact on the structural details of the discrete cluster (Figure 2b). Thus, in the solvate, the alkynyl platinates remain slipped by 1.64 Å. The most significant feature is that the two disparate Pt-Pb distances (2.8663(3) and 3.5834(3) Å) are slightly longer to those found in **1** and, hence, the Pb···Pb separation increases from 5.0893(7) to 5.1842(3) Å (Table 1). In this solvate, **1(acetone)$_2$**·2(Me_2CO), (and also in **3**) as a consequence of the weak Pb···O contacts, the lead center is in a distorted five-coordination, pointing to a lesser stereochemical activity of the lone pair.[17a] The structural analysis was also carried out at 200 and 250K. Unfortunately, the crystals lose not only acetone but also crystallinity at higher temperatures. Between 120 to 250K the most noticeable feature is the slight shortening of the long Pt···Pb, the Pt···Pt and Pb···Pb separations (see Table 1) on increasing the temperature.

Curiously, in the yellow crystals of **2(acetone)$_3$**·and **2(THFMe-2)$_2$**, *all* the solvent molecules incorporated are coordinated to the lead centers, showing shorter Pb-O distances (2.72(1)-2.793(8) Å) to those seen in **1(acetone)$_2$** or **3**. Interestingly, in **2(acetone)$_3$**, two different types of aggregates (Figure 4, labeled as **A** and **B**) are found in the asymmetric unit, which form the extended network showed in Figure S1. The main difference between **A** and **B** is the number of acetone molecules which are bonded to the lead, thus confirming a rather flexible coordination sphere around Pb in these clusters. While in **2A** only one acetone is bonded to each of the Pb (Pb-O = 2.77(1) Å), in **2B** the lead centers interact with two oxygen atoms of two acetones (2.72(1); 2.793(8) Å). In **2B**, owing to the higher coordination number of Pb, the Pb-Pt and Pb-C^{α} bonds (av: Pb-Pt, 3.255 Å; Pb-C^{α} 2.715(8)-2.736(9) Å) are weaker than in **2A** (av. Pb-Pt 3.2045 Å; Pb-C^{α} 2.67(1)-2.726(9) Å) and in the solvent-free clusters. This fact is also reflected, in the metallic core (**2B** displays remarkably longer Pb···Pb and shorter Pt···Pt distances than **2A**, see Table 1), thus suggesting that the stabilization of these clusters involves a synergistic combination between metallophilic Pt···(Pb, Pt^{II}), Pb^{II}··alkynyl and Pb···O(donor) contacts.

In the molecular structure of **2(THFMe-2)$_2$** (Figure S2), although the platinum fragments are eclipsed, as in the acetone cluster **A**, the local environment around the Pb ion is asymmetrical and resembles to the environment of the **1(acetone)$_2$** (see Figure 5). Thus, each Pb(THFMe-2)$^{2+}$ unit (Pb-O = 2.777(7) Å) strongly binds to the Pt and C^{α} atoms of one of the tetraalkynyl platinate units (Pb1-Pt1' = 3.0476(4) Å; Pb-C^{α} = 2.571(6), 2.673(7) Å), while the bond lengths with the other platinum-alkynyl fragment are quite long (Pb-Pt = 3.4898(4); Pb-C^{α} = 2.784(6), 2.801(5) Å), contrasting with the relative symmetrical environment of Pb in **2A** (Pb-C^{α} 2.67 to 2.736 Å). A detailed insight of the bond lengths clearly points that the stereochemical active lone pair is located opposite to the Pb···Pt-C10 vector.[17a]

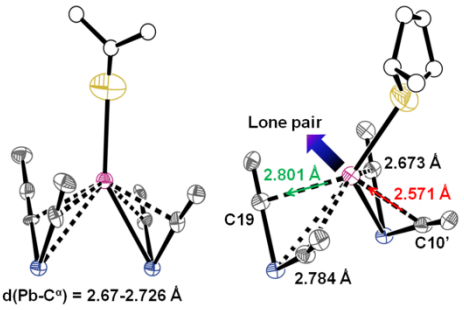

Figure 5. Coordination sphere of Pb^{II} in **2A**: [Pt_2Pb_2(C≡CC_6H_4OMe-3)$_8$]·2(Me_2CO) **2(acetone)$_2$** (left) and [Pt_2Pb_2(C≡CC_6H_4OMe-3)$_8$]·2(THFMe-2) **2(THFMe-2)$_2$** (right).

Photophysical properties in solution: The UV-vis electronic absorption data recorded for **1-3** in several solvents are summarized in Table S3 and, as illustration, the absorption spectra of **1-3** in CH_2Cl_2 and those of cluster **1** in different solvents are depicted in Figures 6a and 6b, respectively. The clusters are characterized by two distinct low energy bands (365, 438 nm **1**; 364, 435 nm **2**; 372, 447 nm **3**) that are ascribed, according to TD-DFT studies (see below) to mixed platinum-alkynyl(ML) to cluster(C) ^{1}MLCCT ($Pt/C{\equiv}CR{\rightarrow}Pt_2Pb_2$)/^{1}IL charge transfer transitions. This assignation is consistent with the slight red-shift of these absorptions in complex **3**, having the more electron-donating alkynyl group (C_6H_4OMe-4). As can be seen in Figure 6b, the low energy absorptions are less intense and display a blue-shift in donor solvents, a feature attributed to coordination of solvent molecules to the lead centers with concomitant formation of solvate clusters $[Pt_2Pb_2(C{\equiv}CR)_8S_x]$ ($x \geq 2$), which feature distinctively different electronic and structural characters. The coordination of the solvent molecules reduces the electronic requirements of the dicationic $\{PbS_x\}^{2+}$ units. This presumably weakens the bonding interactions with the alkynyl platinates and also destabilizes the energy of the LUMO. As substantiated by TD-DFT calculations, by increasing the coordination of acetone molecules, the lowest HOMO-LUMO transition is also gradually blue shifted (see S.I.), increasing somewhat its intraligand character with simultaneous decreasing of the metallic parentage.

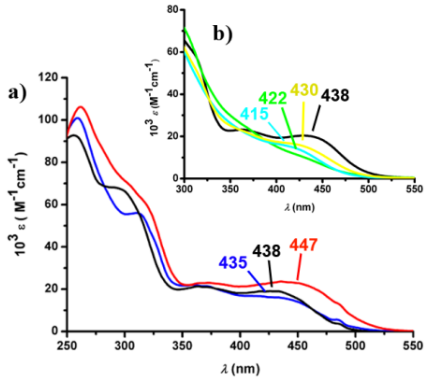

Figure 6. (**a**) Absorption spectra of **1** (black), **2** (blue) and **3** (red) in CH_2Cl_2 (10^{-5} M). (**b**) Absorption spectra of **1** in CH_2Cl_2 (black), acetone (yellow), THFMe-2 (green) and CH_3CN (light blue) (10^{-5} M).

The emission data in solution are compiled in Table S4. All three clusters display unstructured emission bands in frozen CH_2Cl_2 with peak maxima following the energy trend **2** (564 nm) > **1** (580 nm) > **3** (591 nm) which resembles the absorption maxima (see Figure S3). These long-live emissions are assigned to a mixed metal-ligand to cluster/intraligand charge transfer excited state ^{3}MLCCT/^{3}IL ($Pt(d)/\pi(C{\equiv}CR){\rightarrow}Pt_2Pb_2$ /($\pi\pi^*$, C≡CR) on the basis of theoretical calculations. By increasing the temperature the intensity of the emissions gradually decreases exhibiting a slight red shift for **1** and **3**, the two only still weakly emissive at 298K (590 nm **1**; 606 nm **3**).

Photophysical properties in solid states: The photophysical behavior of all clusters in the solid state has also been investigated. The detailed data are compiled in Table 2 and illustrative examples are given in Figures 7-9 and in the Supporting. The orange aggregates **1-3**, free of CH_2Cl_2 as confirmed by NMR, are characterized by a distinctive low energy feature spanning the range 400-490 nm with long tails up to 550 nm (**1**, **2**) or 650 nm for **3** (Figure 7 for **2** and S3 for **1** (**a**) and **3** (**b**)). Upon excitation (λ_{ex} > 320 nm) they exhibit orange-red luminescence centered at 610-615 nm which slightly blue shift at 77K (600-613 nm). In all three clusters the emission is slightly red shifted in relation that seen in glassy solution (564-591 nm). However, the maxima trend is different **3** (600 nm) > **2** (604 nm) > **1** (613 nm) to that observed in glassy state. In attempting to rationalize these observations, it should be noted that the emitting state of these aggregates has strong Pt_2Pb_2 metallic contribution, displaying *bonding Pb-Pb character* and a remarkable *shortening of the Pb···Pb separation* upon photoexcitation. As confirmed by X-ray due to the presence of extended intermolecular Pb···O(Me) contacts, not only the average Pt-Pb bond lengths, but also the Pb···Pb, separation are larger in **3** than in **1** (Pt-Pb 3.22 Å; Pb···Pb 5.36 Å **3** *vs.* Pt-Pb 3.19 Å; Pb···Pb 5.09 Å in **1**). Therefore, the unexpectedly blue-shifted emission of **3** in relation to that of unsolvated **1** and **2** might be tentatively related to the presence of a larger intermetallic Pb···Pb distance in **3**.

Table 2: Luminescent data for complexes **1-3** in the solid state.

	298K				77K
Complex	$\lambda^{max,\,em}$/nm [τ/μs]	ϕ/%	$10^3 k_r/s^{-1}$[a]	$10^3 k_{nr}/s^{-1}$[b]	$\lambda^{max,\,em}$/nm [τ/μs]
1	615 [10.2±0.1]	4.1	4.0	94	613 [14.9±0.3]
1(ground)	625 [12.0±0.5]				
1(acetone)	565 [11.2±0.6]	20.5	18	71	550 [7.9±0.5]
1(THFMe-2)	542 [4.9±0.4]	19.1	39	170	504 [6.3±0.2]
1(CH_3CN)	533 [7.8±0.5]	10.7	14	120	521 [6.1±0.2]
2	613 [9.6±0.2]	8.0	8.3	96	604 [10.1±0.3]
2(ground)	630*br* [10.5±0.9]				
2(acetone)	564 [10.0±0.4]	36.2	36	64	548 [8.7±0.2]
2(THFMe-2)	555 [4.8±0.2]	32.1	67	140	535 [5.6±0.2]
2(CH_3CN)	525 [9.1±0.5]	24.6	27	83	490[7.9±0.1]
3	610 [11.2±0.4]	6.5	5.8	84	600 [10.5±0.5]
3(ground)	630*br* [13.0±0.2]				

[a] $k_r = \phi/\tau$. [b] $k_{nr} = 1/\tau(1-\phi)$

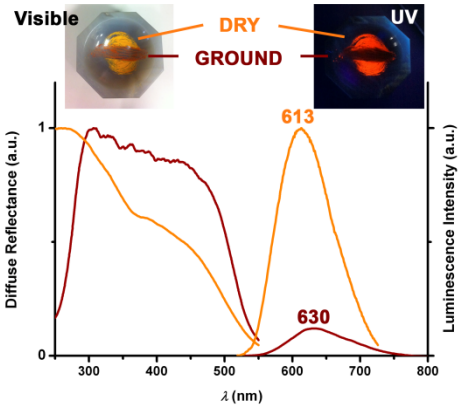

Figure 7. Diffusse Reflectance and emission spectra of **2** (orange) and **2(ground)** (dark-red), together with photographs of both samples under ambient and UV light.

The local environment around the {Pb···Pb} unit plays a decisive role on the excited state and seems to be decisive in their dynamic behavior as dual-responsive luminescent materials. Thus, interesting changes to mechanical grinding were observed for all **1**-**3** clusters, whereas only **1** and **2** showed additionally vapor-stimuli response. As it is illustrated in Figure 7 for **2**, the color and the corresponding emission of the three clusters can be reversibly switched by mechanical forces. Upon grinding they display a color change to deep red, whereas a striking red shift and decrease in the intensity of the emission are observed. The absorption spectra of the pressed powders significantly differed (for **2** dark-red line *vs.* orange line in Figure 7), indicating that the modification in the emission spectra (Table 2) is related to structural changes. Interestingly, the initial orange solids are slowly recovered on standing (ca. 24h) or in a ca. 8h. by exposure to CH_2Cl_2 or Et_2O vapors. This behavior contrasts with the typical grinding/heating cycle observed in most piezochromic organic molecules. It should be noted that mechanochromic materials are attracting significant interest for both fundamental research and practical applications..[19c, 27] To date this phenomenon is well documented in organic molecules [20a, 28] and only a few metal complexes have been recently reported[20, 27, 29] to undergo changes (mainly in the emission) under mild pressure. The responses have been attributed to induced disruptions of intermolecular M···M contacts, interligand π···π stacking or a change in the molecular conformation when grinding.[27, 29] In these Pt_2Pb_2 systems not only small modifications in intermetallic and lead-alkynyl bonding interactions could be responsible but also in the platinate fragments that form secondary contacts between molecules. Indeed, the remarkable quenching and slight red-shift observed in our homoleptic Pt_2Pb_2 systems under pressure could be related, to some extent, with a certain degree of planarization of the Pt fragments including the aromatic groups. This structural change could increase the conjugation in the Pt-C≡CR units, resulting in a red shift in the emission spectra an, also favoring the intermolecular π···π interactions, which are known to cause self-quenching.

The behavior of these clusters towards several organic vapors was also examined. As is illustrated in Figure 8 for **2** and detailed in Table 2, we have found that clusters **1** and **2** show interesting reversible changes in their color (from orange to yellow) and emission (orange to green) when they are exposed to moderate donors such as acetone, THFMe-2 or CH_3CN vapors. The structural changes induced by the absorption of these solvents are revealed in their corresponding UV-vis diffuse reflectance and emission spectra. As shown in Figure 7 for **2** and S4 for **1**, after exposing the solids to these solvents the low energy feature underwent a remarkable blue shift (eg for **1** ~425 acetone; ~430 nm THFMe-2; ~415 CH_3CN). These changes were accompanied by a significant enhancement of photoluminescence intensity with concomitant distinct blue-shits in relation to the free solvent solids. In both clusters (Figure 8 for **2**) the emission maxima follows the sequence: CH_3CN (533 **1**, 525 nm **2**) > THFMe-2 (542 **1**, 555 nm **2**) > acetone (565 **1**, 564 nm **2**) *vs.* dry solids (615 **1**, 613 nm **2**) and, interestingly, the emission displays a remarkable *rigidochromism* upon lowering the temperature to 77K (521 **1**, 490 nm **2** CH_3CN; 504 **1**, 535 nm **2** THFMe-2; 550 **1**, 548 nm **2** acetone). It is worth noting that the solvent uptake as much as the color and luminescent response is extraordinarily fast, and occurs in seconds depending on the solvent and the methodology of the exposure. As is illustrated by Figure 9 for the acetonitrile solvate **2**·$(CH_3CN)_x$, the dynamic recovery of the initial color and emission (attested up to 5 cycles) takes place without external vacuum in relatively short times (1-3 h depending on the solvent).

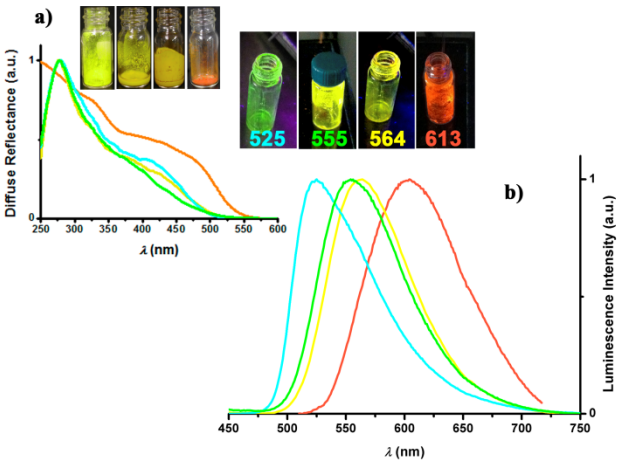

Figure 8. Diffuse reflectances (**a**) and emission spectra (**b**) of complex **2**: dry solid (orange line) and exposed to vapor of acetone (yellow), THFMe-2 (green) and CH_3CN (light blue) together with photographs under ambient and UV light.

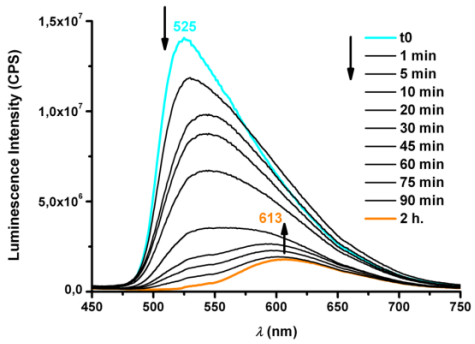

Figure 9. Emission spectra of solvate **2**·S_x (S = CH_3CN) (light blue line) recorded at different time intervals during its drying by air exposure (black lines). After 2 h. (orange line) the emission of **2** is recovered.

Although several factors could likely be involved in the observed changes, including the size of the vapor molecules, the X-ray structures of the acetone and THFMe-2 solvates commented before allow us to suggest that the driven force that presumably causes the greatest impact is related to the formation/rupture of Pb-solvent bonding contacts with simultaneous formation of the solvate clusters. As noted before, in these solvates the intermetallic distances are presumably larger than in free solvent **1**-**3**, in particular the Pb···Pb separation, provoking a destabilization of the ^{3}MLCCT excited state and a slight increase of the ^{3}IL(C≡CR) contribution, as revealed by TDDFT calculations (see below). In the optimized excited state T^1 the Pb···Pb separation of the Pt_2Pb_2 metallic core is remarkably shortened in relation to S^0, and this effect may be also related to the observed red-shift upon increasing the temperature. In fact, the most relevant structural feature observed in **1(acetone)$_2$** by increasing the temperature, before the crystallinity and the acetone are lost (from 120K to 250K), is a slight shortening of the largest of the Pt···Pb distance and of the transannular Pb···Pb separation (see Table 1). As noted in Table 2, the coordination of solvent molecules induces a larger increase in the k_r in relation to k_{nr}, thus explaining

the increase in the quantum yields. In the solvate **1(acetone)$_2$** the calculated k_{nr} is reduced in relation to free solvent **1**, presumably due to the larger separation between clusters, as revealed by X-ray, what seems to be important to decrease excited state quenching patways.

In contrast to this behavior, **3** did not show any vapochromic or vapoluminescence response when exposed to vapors, or even drops of acetone, THFMe-2, or CH_3CN. As noted above, this behavior might be attributed to the electronic and structural effects caused in the Pb centers and in the lattice, respectively, by the presence of intermolecular Pb···O(OMe) secondary contacts. Indeed, these contacts leave no channels or voids close to the Pb^{II} ions, which are presumably required to allow the easy migration of the donor solvent towards the target environment of the Pb center. Interestingly, whereas ethanol did not cause any vapor response in any of the clusters, the three products decompose with formation of a black residue under triethylamine vapors. Furthermore, an *irreversible* effect was observed upon exposure of **1**-**3** to a strong donor solvent such as dimethylsulphoxide (dmso), that causes a dramatic color change from orange to very pale-yellow and a perceivable quenching of the luminescence. The exact nature of these materials together with further reactivity studies of these clusters towards other donor ligands are under investigation.

Computational Studies. In order to get insight into the photophysics of these complexes, theoretical calculations were performed for the free solvent clusters **2** and **3** and for the two solvate molecules **2(acetone)$_2$** (**2A**) and **2(acetone)$_4$** (**2B**). Their S^0 and also the T^1 of **2** and **2A**, geometries were optimized at the PBE0/LanL2DZ(Pt)/6-31G**(ligand atoms) level. The most important geometrical parameters (bond lengths and angles) are listed in Table S5. Detailed orbital compositions and electron-density contours are detailed in Table S6 and Figures S6 and S7.

Calculations (state S^0) correctly reproduce the parallel and eclipsed disposition of the platinum fragments, and predict the geometrical parameters in the metallic core in relatively good agreement with the X-ray structures. For instance, the asymmetric Pt-Pb bonding distances and the relatively short (Pt···Pt) and long (Pb···Pb) *transannular* lengths, which lead to acute Pt-Pb-Pt and wide Pb-Pt-Pb angles, are similar to those of X-ray (Pt-Pb-Pt/Pb-Pt-Pb: Calculated 75.79/104.20° **2A**; 74.35/105.65° **3** *vs.* X-ray data 72.64/107.36° **2A**; 67.47/112.53° **3**). For **2** and the two solvates **2A** y **2B**, calculations predict a gradual shortening of the Pt···Pt distance and simultaneous elongation of the Pb···Pb separation in the metallic core by increasing the number of acetones bonded to the Pb center, thus reflecting the tendency observed in the structures on going from **2A** to **2B** (and also from **1** to **1(acetone)$_2$**). The NBO analysis of Pb^{II} (Table S8) reveals a remarkable gradual decrease of the p contribution on the lead lone pair orbital, caused by the coordination of acetone molecules (S^0: **3** 4.11%, **2** 4.04% >> **2A** 1.98% > **2B** 1.63%). This is in accordance with the final formation of a more holodirected environment.

According to orbital composition (Table S6), for all clusters, the HOMOs (from HOMO to HOMO-8) are mainly centered on the platinum alkynyl fragments with a predominant ligand contribution. By contrast, the LUMOs have a strong metallic contribution (for example for **3** Pb 36%, Pt 20%, C≡CC_6H_4OMe-4 43%), showing primarily Pb···Pb bonding character in all cases, according to electron density surfaces. The binding of the acetone molecules to the Pb^{II} centers in **2** is reflected in a slight and gradual decrease in the contribution of the lead, therefore increasing the contribution of the ligand (Pb/Pt/C≡CR(%): 35/20/45 **2**; 30/22/47 **2(acetone)$_2$**; 27/20/51 **2(acetone)$_4$**).

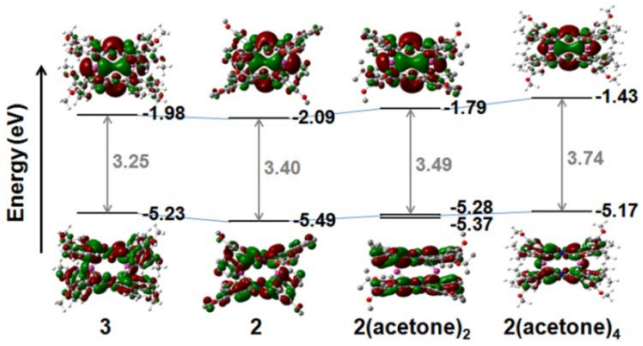

Figure 10. Energy level diagrams including the energy gaps and contour plots of HOMO and LUMO for the studied complexes.

Time Dependent (TD-DFT) calculations (Table S7) in gas phase show that the lowest-energy transition electronic transition ($S^0 \rightarrow S^1$) has a strong platinum-ligand to cluster charge transfer with some intraligand character (MLCCT/IL). By illustration the calculated HOMO and LUMO energy gaps are compared in Figure 10. The energy of the HOMO increases in a larger extension than the LUMO by passing from **2** to **3** due to the best conjugation of the methoxy substituent in *para* position, thus decreasing the value the calculated lowest energy absorption (460 **2**; 482 nm **3**, Table S7) in agreement with the experimental trend. The binding of one (or two) solvent molecules to the Pb decreases its electrophilicity, increasing the energy of the LUMO and the gap of the transitions. The lowest-energy absorptions calculated for the acetone solvates (408 **2B**; 432 **2A** *vs.* 460 nm **2**) agree with the blue shifts observed in the diffuse reflectance spectra.

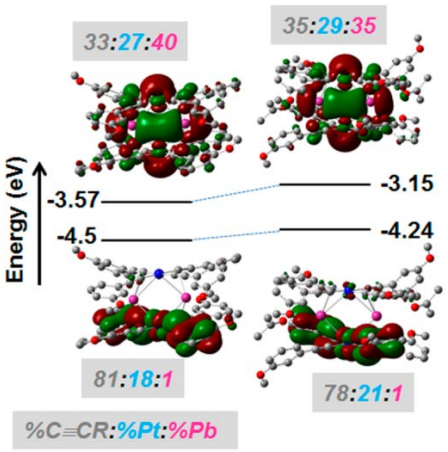

Figure 11. Energy levels (eV) and contour plots of HSOMO and LSOMO calculated for the optimized state T^1 of **2** (left) and **2A** (right).

As representative examples, the optimization of the triplet state geometry T^1 was carried out for **2** and **2A.** (Table S4 and Figure 11). The T^1 geometries show a remarkable symmetrization of the metallic core for both clusters in relation to the corresponding

ground state (S^0). As is illustrated in Figure 12 for **2A,** the longest Pt-Pb distance found in the S^0 is reduced giving rise a final more symmetric Pt_2Pb_2 core (angles at Pt and Pb are comparable) in which the transannular Pt···Pt separation increases whereas the Pb···Pb decreases remarkably (4.960 to 4.476 Å for **2A** and 4.976 to 4.340 Å for **2**). Comparison of the changes between S^0 and T^1 for key geometrical parameters (Table S4) reveals that distortion is larger in the free solvent **2** than in the solvate **2A**, which could, in part, provide a more adequate channel for easy deactivation accounting for the lower observed emission quantum yield (0.36 **2A** *vs.* 0.08 **2**).The lowest energy emissions calculated $\Delta E_{T1\text{-}S0}$ at 551 nm (**2**) and 536 nm **2A**, respectively, agree qualitatively with the experimental data (613 nm **2** and 564 nm **2A**). As can be seen in Figure 11, the composition of the singly occupied orbitals are centered in the metallic core (HSOMO) and the Pt-alkynyl (LSOMO) respectively, suggesting a ^{3}MLCCT/^{3}IL(Pt(d)/π(C≡CR)→Pt_2Pb_2/(ππ*,C≡CR) transition for the emission.

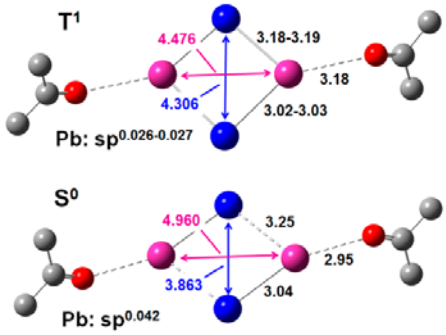

Figure 12. Schematic view of the most relevant geometrical parameters for S^0 and T^1 of **2(acetone)$_2$**.

Conclusions

In summary, we report an unusual series of luminescent homoleptic clusters [Pt_2Pb_2(C≡CR)$_8$] (R = Tol **1**, C_6H_4OMe-3 **2**, C_6H_4OMe-4 **3**) which represents the first examples of platinum-lead complexes featuring a rare planar rhomboidal Pt_2Pb_2 framework. The clusters display a sandwich type structure with the two naked Pb^{2+} connecting the alkynyl platinates by two distinct Pt-Pb bonds and rare Pb···alkynyl bonding interactions. The crystal structures of **1**·CH_2Cl_2 and **3**·2CH_2Cl_2 has allowed us to rationalize their contrasting behavior towards solvent vapors and the distinct photophysical properties in solid state. Thus, in **1**·CH_2Cl_2 the presence of empty channels limited by Pb centers accounts of its fast response to vapors; however, in **3**·2CH_2Cl_2 the presence of secondary intermolecular Pb···O(OMe) originates a more compact lattice that likely prevents the solvent uptake. It has been found that in donor solvents the lead centers easily increase its coordination environment with formation of solvate clusters [Pt_2Pb_2(C≡CR)$_8$·S_x] (x ≥ 2), which alters the electronic characteristic of the clusters, as demonstrated by UV-Vis spectroscopy and confirmed by crystallography of the solvates **1(acetone)$_2$**·2(Me_2CO), **2(acetone)$_3$** and **2(THFMe-2)$_2$**. Curiously, in **2(acetone)$_3$** all the acetone molecules incorporated in the lattice are associated to the primary coordination sphere of Pb, affording two different aggregates **2A** ([Pt_2Pb_2(C≡CR)$_8$(acetone)$_2$] and **2B** ([Pt_2Pb_2(C≡CR)$_8$(acetone)$_4$]), whose geometrical details support a remarkable flexibility of the central metallic Pt_2Pb_2 core, which is key in their intriguing stimuli-responsive photophysical properties.

The solvent free clusters **1-3** display an orange-red phosphorescence assigned to a mixed Pt_2Pb_2/C≡CR (^{3}MLCCT/^{3}IL) excited state, which, according to calculations, displays a predominant lead metallic contribution and an enhanced Pb···Pb bonding character. Notably the three products undergo a bathochromic shift in color an emission on grinding (mechanochromism), which is rapidly reversed by fuming the samples with CH_2Cl_2 or OEt_2; behavior which was tentatively attributed to small inter and intramolecular structural modifications induced on grinding. Interestingly, **1** and **2** also exhibit a fast and reversible vapochromic response to donor solvents (acetone, THFMe-2 *yellow*; NCMe *green* vs *orange* dry solids). This response is ascribed to a fast creation/disruption of solvate clusters [Pt_2Pb_2(C≡CR)$_8$·S_x] (x ≥ 2) with concomitant electronic and geometrical modifications within the Pt_2Pb_2 core, that are easily accessible by a slight tuning of the stereochemical activity of the lone pair. The binding of solvent molecules to the Pb^{2+} reduces its electrophilicity and also increases the Pb···Pb separation in the metallic core, causing a destabilization of the target orbital and a larger gap of the transitions. Interestingly, all solvates exhibit a remarkable rigidochromism upon lowering the temperature, which is associated to a gradual elongation of the transannular Pb···Pb separation as revealed by Temperature-dependent single crystal X-ray of **1(acetone)$_2$**.

It has been demonstrated that the synergistic combinations of the metallophilic interactions and the effect of the stereoactive lone-pair on the Pb^{2+} cation in these clusters can result in a novel approach to the preparation of multi responsive materials. Considering the well-established structural diversity of lead (II), studies are continuing to prepare novel phosphorescent heterometallic-lead systems that exhibit novel properties and potential applications.

Experimental Section

For detailed experimental procedures and characterization of products, see the Supporting Information. CCDC-958649-958650-958651 (**1(acetone)$_2$**·2(Me_2CO)) at 120, 200 and 250K respectively; CCDC-958652 (**1**·CH_2Cl_2); CCDC-958700 (**2(THFMe-2)$_2$**); CCDC-958701 (**2(acetone)$_3$**); CCDC-958702 (**3**·2CH_2Cl_2) contain the supplementary crystallographic data for this paper. These data can be obtained free of charge from The Cambridge Crystallographic Data Centre via www.ccdc.cam.ac.uk/data_request/cif.

Acknowledgements

This work was supported by the Spanish MICINN (Project CTQ2008-06669-C02-02/BQU) and CESGA for computer support.

[1] a) T. Vlček, *Special issue: Controlling Photophysical Properties of Metal Complexes: Towards Molecular Photonics. Coord. Chem. Rev.* **2011**, *255 (21−22)*, 2399; b) V. Guerchais, L. Ordronneau and H. Le Bozec, *Coord. Chem. Rev.* **2010**, *254*, 2553; c) Z.-N. Chen, N. Zhao, Y. Fan and J. Ni, *Coord. Chem Rev* **2009**, *253*, 1; d) V. W.-W. Yam, *Photofunctional Transition Metal Complexes. Structure and Bonding*, Berlin, **2009**, p; e) S. W. Lai and C.-M. Che, *Top. Curr. Chem.* **2004**, *241*, 27; f) A. F. Rausch, H. H. H. Homeier and H. Yersin, *Top. Curr. Organomet. Chem.* **2010**, *29*, 193; g) P. I. Djurovich and M. E. Thompson in *Vol.* (Ed. H. Yersin), Wiley-VCH, Weinheim, Germany, **2008**, p. 131; h) H. F. Xiang, S. W. Lai, P. T. Lai and C.-M. Che in *Vol.* (Ed. H. Yersin), Wiley-VCH, Weinheim, Germany, p. 259; i) R. C. Evans, P. Douglas and C. J. Winscom, *Coord. Chem Rev* **2006**, *250*, 2093; j) J. H. Olivier, J. Harrowfield and R. Ziessel, *Chem. Commun.* **2011**, *47*, 11176; k) V. W.-W. Yam and K. M.-C. Wong, *Chem. Commun.* **2011**, *47*, 11579; l) C. A. Straussert, M. Mauro and L. De Cola, *Inorg. Phot.* **2011**, *63*, 47.

[2] a) V. W.-W. Yam, K. K.-W. Lo and K. M.-C. Wong, *J. Organomet. Chem.* **1999**, *578*, 3; b) K. M. C. Wang, C. K. Hui, K. L. Yu and V. W.-W. Yam, *Coord. Chem. Rev.* **2002**, *229*, 123; c) V. W.-W. Yam, *J. Organomet. Chem.* **2004**, *689*, 1393; d) J. Forniés and E. Lalinde, *A. Perspective. J. Chem. Soc., Dalton Trans.*

1996, 2587; e) N. J. Long and C. K. Williams, *Angew. Chem., Int. Ed. Engl.* **2003**, *42*, 2586; f) P. Mathur, S. Chatterjee and V. D. Avasare, *Adv. Organomet. Chem.* **2008**, *55*, 201; g) J. R. Berenguer, E. Lalinde and M. T. Moreno, *Coord. Chem Rev* **2010**, *254*, 832 and ref. therein; h) R. Buschbeck, P. J. Low and H. Lang, *Coord. Chem. Rev.* **2011**, *255*, 241; i) A. Díez, E. Lalinde and M. T. Moreno, *Coord. Chem. Rev.* **2011**, *255*, 2426.

[3] a) X. He and V. W.-W. Yam, *Highlight Coord. Chem. Rev.* **2011**, *255*, 2111; b) H. Lang, A. Jakob and B. Milde, *Organometallics* **2012**, *31*, 7661; c) J. C. Lima and L. Rodriguez, *Chem. Soc. Rev.* **2011**, *40*, 5442; d) V. W.-W. Yam and E. C.-C. Cheng, *Chem. Soc. Rev.* **2008**, *37*, 1806; e) W.-Y. Wong, *Coord. Chem Rev* **2007**, *251*, 2400; f) T. C. W. Mak, X.-L. Zhao, Q.-M. Wang and G.-C. Guo, *Coord. Chem Rev* **2007**, *251*, 2311; g) D. Michel, P. Mingos, R. Vilar and D. Rais, *J. Organomet. Chem.* **2002**, *641*, 126; h) V. W.-W. Yam and E. Chung-Chin Cheng, *Top Curr. Chem.* **2007**, *281*, 269.

[4] a) I. O. Koshevoy, C. L. Lin, A. J. Karttunen, J. Jänis, M. Haukka, S. P. Tunik, P. T. Chou and T. Pakkanen, *Chem. Eur. J.* **2011**, *17*, 11456; b) I. O. Koshevoy, Y. C. Chang, A. J. Karttunen, M. Haukka, T. Pakkanen and P. T. Chou, *J. Am. Chem. Soc.* **2012**, *134*, 6564; c) M. C. Blanco, J. Camara, M. C. Gimeno, A. Laguna, S. L. James, M. C. Lagunas and M. D. Villacampa, *Angew. Chem. Int. Ed.* **2012**, *51*, 9777; d) C. Y. Gao, X. He, L. Zhao and M. X. Wang, *Chem. Comm.* **2012**, *48*, 8368; e) A. Himmelspach, M. Finze and S. Raub, *Angew. Chem. Int. Ed.* **2011**, *50*, 2628; f) H. Smichdbaur and A. Shier, *Organometallics* **2010**, *29*, 2; g) X. He, N. Zhu and V. W.-W. Yam, *Dalton Trans.* **2011**, *40*, 9703; h) G. F. Manbeck, W. W. Brennessel, R. A. J. Stockland and R. Eisenberg, *J. Am. Chem. Soc.* **2010**, *132*, 12307.

[5] a) E. S. H. Lam, A. Y. Y. Tam, W. H. Lam, K. M. C. Wong, N. Zhu and V. W.-W. Yam, *Dalton Trans.* **2012**, *41*, 8773; b) J. R. Berenguer, A. Díez, A. García, E. Lalinde, M. T. Moreno, S. Sánchez and J. Torroba, *Organometallics* **2011**, *30*, 1646; c) Q. H. Wei, L. J. Han, Y. Jiang, X. X. Lin, Y. N. Duan and G. N. Chen, *Inorg. Chem.* **2012**, *51*, 11117; d) A. Díez, A. García, E. Lalinde and M. T. Moreno, *Eur. J. Inorg. Chem.* **2009**, 3060; e) B. Gil, J. Forniés, J. Gómez, E. Lalinde, A. Martín and M. T. Moreno, *Inorg. Chem.* **2006**, *45*, 7788 and ref. therein; f) J. Forniés, S. Fuertes, A. Martín, V. Sicilia, E. Lalinde and M. T. Moreno, *Chem. Eur. J* **2006**, *12*, 8253; g) G.-Q. Yin, Q.-H. Wei, L.-Y. Zhang and Z.-N. Chen, *Organometallics* **2006**, *25*, 580.

[6] I. O. Koshevoy, Y. C. Chang, A. J. Karttunen, S. I. Selivanov, J. Jänis, M. Haukka, T. Pakkanen, S. P. Tunik and P. T. Chou, *Inorg. Chem.* **2012**, *51*, 7392.

[7] a) J. R. Berenguer, J. Fernández, B. Gil, E. Lalinde and S. Sánchez, *Inorg. Chem.* **2010**, *49*, 4232; b) J. R. Berenguer, B. Gil, J. Fernández, J. Forniés and E. Lalinde, *Inorg. Chem.* **2009**, *48*, 5250; c) J. Forniés, S. Ibáñez, A. Martín, B. Gil, E. Lalinde and M. T. Moreno, *Organometallics* **2004**, *23*, 3963; d) J. Fernández, J. Forniés, B. Gil, J. Gómez, E. Lalinde and M. T. Moreno, *Organometallics* **2006**, *25*, 2274; e) J. Forniés, J. Gómez, E. Lalinde and M. T. Moreno, *Inorg. Chem.* **2001**, *40*, 5415; f) J. P. H. Charmant, L. R. Falvello, J. Forniés, J. Gómez, E. Lalinde, M. T. Moreno, A. G. Orpen and A. Rueda, *Chem. Commun.* **1999**, 2045.

[8] a) I. Ara, J. R. Berenguer, J. Forniés, J. Gómez, E. Lalinde and R. I. Merino, *Inorg. Chem.* **1997**, *36*, 6461; b) J. R. Berenguer, J. Forniés, J. Gómez, E. Lalinde and M. T. Moreno, *Organometallics* **2001**, *20*, 4847; c) J. P. H. Charmant, J. Forniés, J. Gómez, E. Lalinde, R. I. Merino, M. T. Moreno and A. G. Orpen, *Organometallics* **2003**, *22*, 652; d) J. R. Berenguer, J. Forniés, B. Gil and E. Lalinde, *Chem. Eur. J.* **2006**, *12*, 785; e) Á. Díez, J. Fernández, E. Lalinde, M. T. Moreno and S. Sánchez, *Inorg. Chem.* **2010**, *49*, 11606; f) J. Forniés, S. Fuertes, A. Martín, V. Sicilia, B. Gil and E. Lalinde, *Dalton Trans.* **2009**, 2224.

[9] a) J. Bauer, H. Braunschweig and R. D. Dewhurst, *Chem. Rev.* **2012**, *112*, 4329; b) V. J. Catalano, B. L. Bennet, M. A. Malwitz, R. L. Yson, H. M. Kar, S. Muratidis and S. J. Horner, *Comments Inorg. Chem.* **2003**, *24*, 39; c) D. Heitmann, T. Pape, A. Hepp, C. Mück-Lichtenfeld, S. Grimme and F. E. Hahn, *J. Am. Chem. Soc.* **2011**, *133*, 11118; d) H. Braunschweig, A. Damme, R. D. Dewhurst, F. Hupp, J. O. C. Jiménez-Halla and K. Radacki, *Chem. Comm.* **2012**, *48*, 10410; e) S. Way, G. Garzon, C. King, J. C. Wang and J. P. J. Fackler, *Inorg. Chem.* **1989**, *28*, 4623; f) V. J. Catalano, B. L. Bennett and B. C. Noll, *Chem. Commum.* **2000**, 1413; g) A. L. Balch, E. Y. Fung, J. K. Nagle, M. M. Olmstead and S. P. Rowley, *Inorg. Chem.* **1993**, *32*, 3295; h) I. Ara, L. R. Falvello, J. Forniés, J. Gómez-Cordón, E. Lalinde, R. I. Merino and I. Usón, *J. Organomet. Chem.* **2002**, *663*, 284.

[10] J. R. Berenguer, A. Díez, J. Fernández, J. Forniés, A. García, B. Gil, E. Lalinde and M. T. Moreno, *Inorg. Chem.* **2008**, *47*, 7703.

[11] a) J. Parr in *Vol. 3* (Ed. G. F. R. Parkin), Elsevier Pergamon, Boston, **2004**, p. 545; b) M. Weindenbruch in *Vol. 3* (Ed. C. E. Housecroff), Elsevier Ltd., New Haven, USA, **2007**, p. 855.

[12] G. Tang, C. L. Lin, L. Luo and W. Chen, *J. Lumin.* **2010**, *130*, 821.

[13] a) M. J. Katz, P. M. Aguiar, R. J. Batchelor, A. A. Bokov, Z. G. Ye, S. Kroeker and D. B. Leznoff, *J. Am. Chem Soc.* **2006**, *128*, 3669 and ref. therein; b) M. B. J. Sigman and B. A. Korger, *J. Am. Chem. Soc.* **2005**, *127*, 10089; c) M. J. Katz and D. B. Leznoff, *J. Am. Chem. Soc.* **2009**, *131*, 18435.

[14] R. Newnham, *MRS Bull* **1997**, *XXII*, 20.

[15] C. B. Murray, S. Sun, W. Gaschler, H. Doyle, T. A. Betley and C. R. Kaga, *I. B. M. J. Res. Dev.* **2001**, *45*, 47.

[16] S. P. Zhao and X. M. Ren, *Dalton Trans.* **2011**, *40*, 8261 and ref. therein.

[17] a) L. Shimoni-Liuny, J. P. Glusker and C. W. Bock, *Inorg. Chem.* **1998**, *37*, 1853; b) R. L. Davidovich, V. Stavila, D. V. Marinin, E. F. Voit and K. H. Whitmic, *Coord. Chem. Rev.* **2009**, *253*, 1316; c) R. L. Davidovich, V. Stavila and K. H. Whitmire, *Coord. Chem. Rev.* **2010**, *254*, 2193; d) C. Gourlaoven, H. Gérard, J. P. Piquemal and O. Parised, *Chem. Eur. J.* **2008**, *14*, 2730; e) B. J. Greer, V. K. Michaelis, M. J. Katz, D. B. Leznoff, G. Schreckenbach and S. Kroeker, *Chem. Eur. J* **2011**, *17*, 3609.

[18] Hemidirected structures have a void in the coordination sphere of Pb^{II} which is occupied by the stereochemically active lone pair. This type of coordination always occur with low coordination numbers (less than 6) and can be also observed for complexes with higher coordination numbers (6-8). Symetrical holodirected structures are usually found with high coordination numbers (9-10).

[19] a) Q. Zhao, F. Li and C. Huang, *Chem. Soc. Rev.* **2010**, *39*, 3007; b) X. Zhang, B. Li and Z. N. Chen, *J. Mater. Chem.* **2012**, *22*, 11427; c) G. G. Shan, H. B. Li, H. T. Cao, D. X. Zhu, P. Li, Z. M. Su and Y. Liao, *Chem. Comm.* **2012**, *48*, 2000; d) O. S. Wenger, *Chem. Rev.* **2013**, *113*, 2013; e) Y. Hong, J. W. Y. Lam and B. Z. Tang, **2009**, 4332.

[20] a) R. J. Wojtecki, M. A. Meador and S. J. Rowan, *Nat. Mat.* **2011**, 14; b) X.-C. Shan, H.-B. Zhang, L. Chen, M. Y. Wu, F.-L. Jiang and M.-C. Hong, *Cryst. Growth Des.* **2013**, *13*, 1377; c) T. Wen, D.-X. Zhang, J. Liu, R. Lin and J. Zhang, *Chem. Commun.* **2013**, *49*, 5660; d) X.-C. Shan, F.-L. Jiang, L. Chen, M. Y. Wu, P. Pan, X.-Y. Wan and M.-C. Hong, *J. Mater. Chem. C.* **2013**, *1*, 4339; e) A. Laguna, T. Lasanta, J.-M. Lopez-de-Luzuriaga, M. Monge, P. Naumov and M. E. Olmos, *J. Am. Chem. Soc.* **2010**, *132*, 456; f) S. Perruchas, X. F. Le Goff, S. Maron, I. Maurin, F. Guillen, A. García, T. Gacoins and J.-P. Boilot, *J. Am. Chem. Soc.* **2010**, *132*, 10967; g) J. Wang, J. Mei, R. Hu, J. Z. Sun, A. Qin and B. Z. Tang, *J. Am. Chem. Soc.* **2012**, *134*, 9956.

[21] A central triplet (1:3.5:1) of the expected quintuplet (1:17.2:60.7:17.2:1) arising from the subspected of the more abundant isotopomeric combinations (^{195}Pt/Pt Pb_2 26.8%; ^{195}Pt/Pt ^{207}Pb/Pb 15.7%; $^{195}Pt_2$ Pb_2 6.8%; $^{195}Pt_2$ ^{207}Pb/Pb 4%; ^{195}Pt/Pt $^{207}Pb_2$ 2.29%).

[22] V. G. Albano, C. Castellari and M. Monari, *Organometallics* **1995**, *14*, 4213.

[23] a) R. Usón, J. Forniés, L. R. Falvello, M. A. Usón and I. Usón, *Inorg. Chem.* **1992**, *31*, 3697; b) J. M. Casas, J. Forniés, A. Martín, V. M. Orera, A. G. Orpen and A. Rueda, *Inorg. Chem.* **1995**, *34*, 6514; c) J. R. Berenguer, E. Lalinde, A. Martín, M. T. Moreno, S. Ruiz, S. Sánchez and H. R. Shahsavari, *Chem. Commun.* **2013**, 5067.

[24] M. Mantina, A. C. Chamberlin, R. Valero, C. J. Cramer and D. G. Truhlar, *J. Phys. Chem. A.* **2009**, *113*, 5806.

[25] N. Komiya, N. Itami and T. Naota, *Chem. Eur. J.* **2013**, *19*, 9497.

[26] B. M. Anderson and S. K. Hurst, *Eur. J. Inorg. Chem.* **2009**, 3041.

[27] a) X. Zhang, Z. Chi, Y. Zhang, S. Liu and J. Xu, *J. Mater. Chem. C.* **2013**, *1*, 3376; b) Y. Sagara and T. Kato, *Nat. Chem.* **2009**, *1*, 605; c) A. L. Balch, *Angew. Chem. Int. Ed.* **2009**, *48*, 2641.

[28] a) Y. Chi and P.-T. Chou, *Chem. Soc. Rev.* **2010**, *39*; b) S.-J. Yoom and S. Y. Park, *J. Mater. Chem.* **2011**, *21*, 8338; c) K. Nagura, S. Saito, H. Yusa, H. Yamawaki, H. Fujihisa, H. Sato, Y. Shimoikeda and S. Yamaguchi, *J. Am. Chem. Soc.* **2013**, *135*, 10322; d) Y. Dong, B. Xu, J. Zhang, X. Tan, L. Wang, J. Chen, H. Lv, S. Wen, B. Li, L. Ye, B. Zou and W. Tian, *Angew. Chem. Int. Ed.* **2012**, *51*, 10782; e) J. W. Chung, Y. Yon, H. S. Huh, B.-K. An, S.-J. Yoon, S. H. Kim, S. W. Lee and S. Y. Park, *J. Am. Chem. Soc.* **2009**, *131*, 8163.

[29] a) J. Ni, X. Zhang, Y.-H. Wu, L.-Y. Zhang and Z.-N. Chen, **2011**, *17*, 1171; b) T. Tsukuda, M. Kawase, A. Dairiki, K. Matsumoto and T. Tsubomura, *Chem. Commun.* **2010**, *46*, 1905; c) M. G. Babashkina, D. A. Safin, M. Bolte and Y. García, *Dalton Trans.* **2011**, *40*, 8523; d) M. Osaga, I. Kawata, S. Igawa, M. Hashino, T. Fukunaga and D. Hashizume, *Chem. Eur. J.* **2010**, *16*, 12114; e) B.-C. Tzeng, T.-Y. Chang, S.-L. Wei and H.-S. Sheu, *Chem. Eur. J.* **2012**, *18*, 5105; f) G.-G. Shan, H.-B. Li, H.-Z. Sun, D.-X. Zhu, H.-T. Cao and Z.-M. Su, *J. Mater. Chem. C.* **2013**, *1*, 1440.

Received: ((will be filled in by the editorial staff))
Revised: ((will be filled in by the editorial staff))
Published online: ((will be filled in by the editorial staff))

Entry for the Table of Contents

Catch Phrase

Jesús R. Berenguer, Julio Fernández, Belén Gil, Elena Lalinde* and Sergio Sánchez*..... Page – Page

Reversible Binding of Solvent to Naked Pb^{II} Centers in Unusual Homoleptic Alkynyl Based $\{Pt_2Pb_2\}$ Clusters

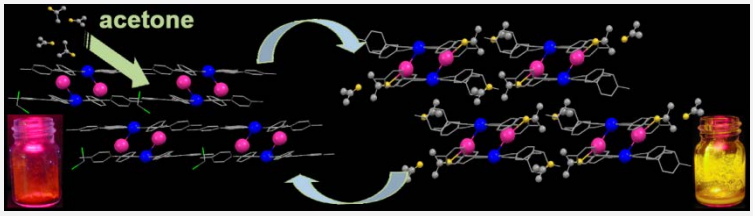

Brigth emissive sandwich-type Lead-Platinum clusters with a dynamic metallic core sensitive to grinding and donor solvent vapors are described. The vapochromic response is due to a fast creation/disruption of Pb-solvate clusters $[Pt_2Pb_2(C{\equiv}CR)_8S_x]$ (S = donor solvent) with associated electronic changes. These changes entail a slight tuning of the stereochemical activity of the lone pair of lead with a concomitant modification of the excited state, having strong Pb-Pb contribution.